ENVIRONMENTAL RESEARCH
LETTERS

LETTER · OPEN ACCESS

Multi-scale observations of mangrove blue carbon ecosystem fluxes: The NASA Carbon Monitoring System BlueFlux field campaign

To cite this article: Benjamin Poulter *et al* 2023 *Environ. Res. Lett.* **18** 075009

IOP Publishing Environ. Res. Lett. 18 (2023) 075009 https://doi.org/10.1088/1748-9326/acdae6

ENVIRONMENTAL RESEARCH
LETTERS

OPEN ACCESS

RECEIVED
16 January 2023

REVISED
27 March 2023

ACCEPTED FOR PUBLICATION
2 June 2023

PUBLISHED
10 July 2023

LETTER

Multi-scale observations of mangrove blue carbon ecosystem fluxes: The NASA Carbon Monitoring System BlueFlux field campaign

Benjamin Poulter[1,*], Francis M Adams-Metayer[2], Cibele Amaral[3], Abigail Barenblitt[1], Anthony Campbell[1], Sean P Charles[4], Rosa Maria Roman-Cuesta[5], Rocco D'Ascanio[2], Erin R Delaria[1,10], Cheryl Doughty[1], Temilola Fatoyinbo[1], Jonathan Gewirtzman[2], Thomas F Hanisco[1], Moshema Hull[2], S Randy Kawa[1], Reem Hannun[6], David Lagomasino[4], Leslie Lait[7], Sparkle L Malone[2], Paul A Newman[1], Peter Raymond[2], Judith A Rosentreter[2,8,11,12], Nathan Thomas[1], Derrick Vaughn[2], Glenn M Wolfe[1], Lin Xiong[4], Qing Ying[9] and Zhen Zhang[9]

[1] NASA Goddard Space Flight Center, Earth Sciences Division, Greenbelt, MD 20771, United States of America
[2] Yale School of the Environment, Yale University, New Haven, CT, United States of America
[3] Earth Lab, Cooperative Institute for Research in Environmental Sciences, University of Colorado, Boulder, Boulder, CO 80303, United States of America
[4] Integrated Coastal Programs, East Carolina University, Wanchese, NC, United States of America
[5] Wageningen University & Research, Laboratory of Geo-Information Science and Remote Sensing, 6708PB Wageningen, The Netherlands
[6] Department of Geology and Environmental Science, University of Pittsburgh, Pittsburgh, PA 15260, United States of America
[7] Science Systems and Applications Inc., Lanham, MD, United States of America
[8] Yale Institute for Biospheric Studies, Yale University, New Haven, CT, United States of America
[9] Earth System Science Interdisciplinary Center, University of Maryland, College Park, MD 20742, United States of America
[10] Oak Ridge Associated Universities, Oak Ridge, TN 37830, United States of America
[11] Yale Institute for Biospheric Studies, Yale University, New Haven, CT 06520, United States of America
[12] Centre for Coastal Biogeochemistry, Faculty of Science and Engineering, Southern Cross University, Lismore, NSW 2480, Australia
[*] Author to whom any correspondence should be addressed.

E-mail: benjamin.poulter@nasa.gov

Keywords: nature-based climate solutions, natural climate solutions, climate mitigation, carbon dioxide, methane

Abstract

The BlueFlux field campaign, supported by NASA's Carbon Monitoring System, will develop prototype blue carbon products to inform coastal carbon management. While blue carbon has been suggested as a nature-based climate solution (NBS) to remove carbon dioxide (CO_2) from the atmosphere, these ecosystems also release additional greenhouse gases (GHGs) such as methane (CH_4) and are sensitive to disturbances including hurricanes and sea-level rise. To understand blue carbon as an NBS, BlueFlux is conducting multi-scale measurements of CO_2 and CH_4 fluxes across coastal landscapes, combined with long-term carbon burial, in Southern Florida using chambers, flux towers, and aircraft combined with remote-sensing observations for regional upscaling. During the first deployment in April 2022, CO_2 uptake and CH_4 emissions across the Everglades National Park averaged -4.9 ± 4.7 μmol CO_2 m^{-2} s^{-1} and 19.8 ± 41.1 nmol CH_4 m^{-2} s^{-1}, respectively. When scaled to the region, mangrove CH_4 emissions offset the mangrove CO_2 uptake by about 5% (assuming a 100 year CH_4 global warming potential of 28), leading to total net uptake of 31.8 Tg CO_2-eq y^{-1}. Subsequent field campaigns will measure diurnal and seasonal changes in emissions and integrate measurements of long-term carbon burial to develop comprehensive annual and long-term GHG budgets to inform blue carbon as a climate solution.

1. Introduction

Blue carbon is a key component in climate mitigation strategies that aim to reduce atmospheric carbon dioxide (CO_2) concentrations through coastal vegetated and open-ocean long-term carbon removal (Mcleod *et al* 2011, Macreadie *et al* 2021). By definition, blue carbon is the long-term removal of atmospheric CO_2 through burial processes taking place in soil sediments (Nellemann *et al* 2009, Duarte *et al* 2013). At global scales, blue carbon forms part of the land-mitigation portfolio that could enable the Paris Agreement goal of keeping warming below 2.0 °C and for achieving net-zero greenhouse-gas (GHG) emissions (Roe *et al* 2019). The high primary productivity of mangroves, salt marshes, and sea grasses, combined with high restoration and conservation potentials, is estimated to store on order of an additional 1–5 $PgCO_2$-eq yr^{-1} over present-day rates (Griscom *et al* 2017). Given the wide range of services that coastal ecosystems provide and combined with their historical losses from land-use change (Goldberg *et al* 2020), blue carbon could incentivize coastal restoration and protection through carbon financing (Zeng *et al* 2021) and help avoid projected losses of coastal ecosystems in the future (Adame *et al* 2021).

Nature-based climate solutions (NBSs) aim to enhance carbon uptake and ecosystem co-benefits simultaneously (Seddon 2022), yet carbon-focused activities pose risks from social and physical science perspectives (Macreadie *et al* 2021, Williamson and Gattuso 2022). Concerns about trade-offs between carbon-based management with biodiversity, water resources, food security and energy balance need thorough investigation (IPCC 2019). Unique to blue carbon is that coastal vegetated ecosystems can also emit methane due to anoxic soils and the presence of methanogenic archaea. Methane (CH_4) is a potent GHG with a 20 and 100 year global warming potential (GWP_{20} and GWP_{100}) 81.2 and 27.9 times greater than CO_2 (Forster *et al* 2021); thus, the climate mitigation potential of coastal wetlands must be assessed by considering both CO_2 removal via long-term burial and CH_4 emissions (Rosentreter *et al* 2018b). Measurements of these two trace gases and long-term burial rates are sparse, however, with observations from soil chambers and flux towers limited to small geographic regions or over short time periods, leading to regional and global budgets that are highly uncertain (Rosentreter *et al* 2021).

Mangrove ecosystems are of particular interest from a blue carbon perspective as they are one of the most productive ecosystems on Earth, with net primary production (NPP) ranging from 1000–2000 g C m^{-2} yr^{-1} (Alongi 2020). While only covering a fraction of the Earth's land surface, 147 359 km^2 (Pete *et al* 2022), they contribute ~210 TgC yr^{-1} to global NPP (Alongi 2014). Much of this carbon becomes stored in short-term biomass or sequestered long-term in soil sediments, with recent lidar and radar estimates of total mangrove carbon stocks estimated around 5.03 PgC (Marc *et al* 2019; and references within ranging from 1.32 to 11.2 PgC). These carbon stocks are concentrated in just a few key geographic regions, e.g. ten countries account for over 70% of total carbon stocks (Marc *et al* 2019), which means that at national scales, mangrove carbon management can play a large role in nationally determined contributions and climate mitigation.

In contrast to CO_2, global fluxes of methane from mangrove ecosystems range from 0.2 to 1.5 Tg CH_4 yr^{-1} (Rosentreter *et al* 2021), a relatively small fraction of total coastal and inland wetland methane emissions (180–431 Tg CH_4 yr^{-1}, Saunois *et al* 2020, Rosentreter *et al* 2021). However, expressed in CO_2-equivalents using the 20 year GWP (GWP_{20}) and GWP_{100}, Rosentreter *et al* (2018) estimated that methane emissions of 6.14 and 2.53 Tg CH_4-CO_2-eq offset about 10%–20% of global mangrove carbon burial (31.3 TgC yr^{-1}). Nitrous oxide (N_2O) can also be emitted by mangrove systems where there is high nitrogen runoff, further reducing climate mitigation potential (Rosentreter *et al* 2021). For CH_4 emissions, considerable variability exists across gradients in climate, species, disturbance history, and from tidal influences on salinity, which affect how well we know the ratio between carbon uptake to methane efflux. For example, based on a synthesis of flux-tower observations, Delwiche *et al* (2021) found mangrove ecosystems to emit ~14.1 g CH_4 m^{-2} yr^{-1}, and from chambers, Rosentreter *et al* (2018b) estimated 1.0–1.9 g CH_4 m^{-2} yr^{-1} (339 ± 106 μmol CH_4 m^{-2} d^{-1}). In general, flux-tower observations tend to show that the range of mangrove methane fluxes are lower than the mean of global annual wetland CH_4 fluxes of 13 ± 2 g CH_4 m^{-2} yr^{-1} (Knox *et al* 2019) and 22 g CH_4 m^{-2} yr^{-1} (Delwiche *et al* 2021).

To address these uncertainties, in 2020, the NASA Carbon Monitoring System (CMS) provided support to establish the BlueFlux field campaign with the objective to develop prototype CO_2 and CH_4 products to inform mangrove restoration and conservation. The BlueFlux field campaign is designed to provide comprehensive measurements of CO_2 and CH_4 fluxes and long-term burial rates across Southern Florida and the Caribbean, with a focus on mangrove forests, their seasonal dynamics, and the adjacent extensive sawgrass marshes and tree 'islands'. Increasing tropical storm frequency and intensity, as well as sea-level rise, is also affecting mangrove productivity, soil carbon, salinity and lateral fluxes, with unknown impacts on the carbon cycle (Taillie *et al* 2020). BlueFlux measurements cover a gradient of 'healthy' mangroves to recently disturbed and dying mangrove 'ghost forests' to help understand any directional change in carbon fluxes from losses

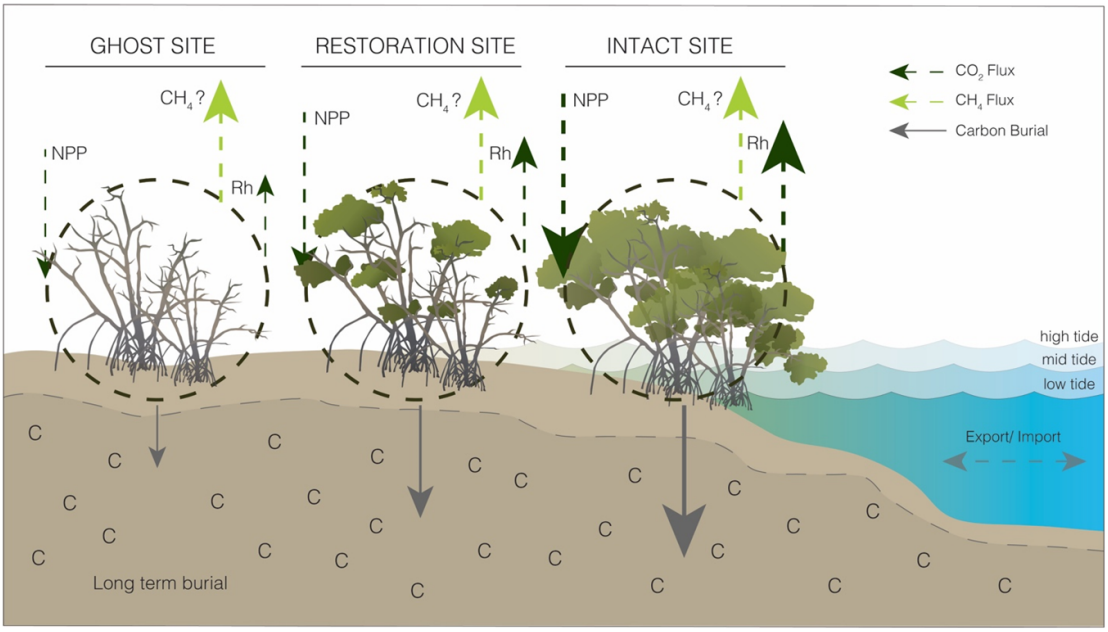

Figure 1. Schematic overview of BlueFlux's objectives to compare and contrast NPP (burial), heterotrophic respiration (Rh) producing CO_2 with methane GHG release across the existing disturbance and recovery gradients in Southern Florida.

and recovery due to change in carbon burial rates and hydroperiod (figure 1).

2. The region: blue carbon in Southern Florida and the Caribbean

BlueFlux covers a geographic domain that includes the Caribbean and Mesoamerican region, and parts of the Gulf of Mexico, the islands of the Caribbean, and the coastal zones of Central and South America (figure 2). The coastal vegetated ecosystems within this region have been extensively impacted by development, hurricanes that cause erosion, and storm surge and mangrove dieback (Sippo *et al* 2018, Taillie *et al* 2020, Lagomasino *et al* 2021), sea-level rise (Parkinson and Wdowinski 2022), and freeze events at the northern range limits (Cavanaugh *et al* 2014, Malone *et al* 2016, Osland *et al* 2019, Goldberg *et al* 2020). These losses of mangroves are already expected to have foregone carbon sequestration opportunities in the range of 100s Tg CO_2-eq yr^{-1} (Adame *et al* 2021).

Three mangrove species grow in the Gulf of Mexico; red mangroves (*Rhizophora mangle*) with their distinctive aerial prop roots; black mangroves (*Avicennia germinans*) that have pneumatophores providing stability and oxygen to roots; and white mangroves (*Laguncularia racemosa*) with a smaller-glands at the leaf base to excrete salt. The distribution of each species is controlled by several factors including geomorphology, tidal connectivity, and soil properties (Snedaker 1982). These factors can also influence the production of GHGs which measurements made in BlueFlux will aim to characterize across all mangrove species and their surrounding soils.

In-situ ground and aircraft measurements target areas within the conterminous USA, and ecosystems in Southern Florida that include a mix of ownerships (i.e. private, state, tribal and Federal). The Everglades and Big Cypress National Parks, which have a long history of biogeochemical research in association with the Florida Coastal Everglades Long-term Ecological Research Network (FCE-LTER, supported by the National Science Foundation), provides linkages with historical and contemporary research activities. The Everglades landscape includes a diversity of wetland (marsh, prairies, swamps) and upland (tree islands and hard wood hammocks) ecosystems that range from short-statured freshwater marsh and marl prairies, to mangrove scrub, and tall riverine mangrove forest along the coast. Several flux towers within the National Park boundaries provide information for both CO_2 and CH_4 exchange for dominant ecosystems (fresh water marsh, freshwater marl prairies, mangrove scrub, and riverine mangrove forest) and data from flux towers in Panama (managed by the Technological University of Panama in the Juan Diaz mangroves) and one in the Yucatan (at Puerto Morelos, Quintana Roo, Alvarado-Barrientos *et al* 2021) will be used for sites outside of the United States.

3. The BlueFlux field campaign

Within the Southern Florida core region, carbon stock and flux measurements are being made to understand how species, disturbance, hydrologic and

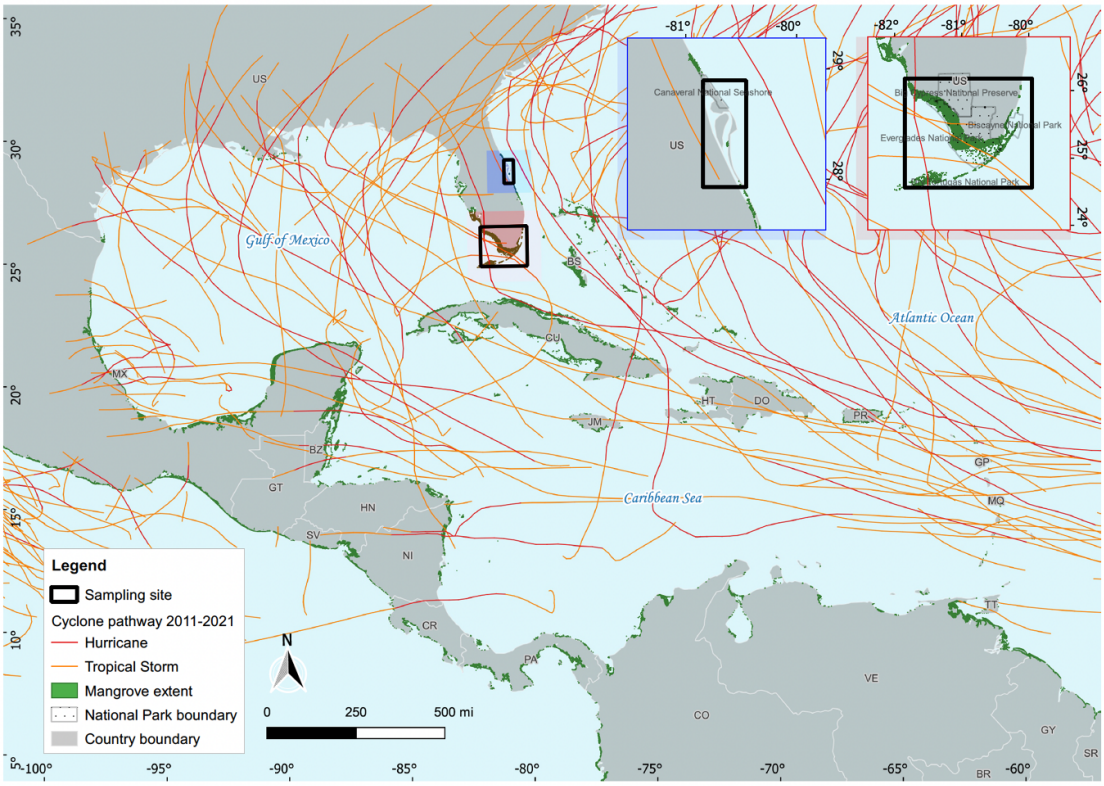

Figure 2. The Gulf of Mexico study region, showing mangrove extent (green) and the paths of tropical storms and hurricanes from 2011–2021 that drive the losses of mangroves through erosion and wind damage. Insets show the areas where the airborne component of BlueFlux will carry out eddy covariance measurements.

climatic gradients explain flux variation. Six field campaigns, consisting of ground-based and airborne-based measurements are planned from 2022 to 2024, with the first three field campaigns successfully carried out in April and October of 2022 and February of 2023. The following sections describe the field campaign and measurements made for (1) forest inventory, (2) forest biomass, (3) species composition, (4) soil and vegetation fluxes, (5) water chemistry, (6) long-term carbon burial, (7) ecosystem fluxes, and (8) data-driven upscaling.

3.1 Ground Measurements

3.1.1. Ground measurements: mangrove forest inventory

Mangrove forest inventory data were collected at locations ranging in forest condition, with a primary focus on recently disturbed, dead, or regenerating mangrove ghost forests caused by recent extreme weather events. This information will be used to estimate plot-level forest wood volume and standing and dead biomass density. At each plot location a 100 m^2 square plot was established, with the center of the plot oriented in the north and south cardinal directions. A global positioning system (GPS) location was recorded at the plot center and at each plot corner using a World Geodetic System 1984 (WGS84) reference coordinate system. All trees taller than 0.5 m were tagged with a unique identity and the diameter and height of the tree were recorded using Diameter-at-Breast-Height (DBH) tape and a hypsometer, respectively. The species and condition (i.e. live or relative decomposition of dead) of each tree was also noted. For plots with seedlings, we identified the species and measured height and basal diameter of each seedling in a 1 m^2 subplot. To record the quantity of debris material on the forest floor, five 10 m transects were laid out every 72° radially starting along the North (0°) cardinal direction. At every 1 m interval along each transect, the size of any fallen woody debris that intersected the line was recorded. Within each of the 1 m intervals, a tally of the size of any fallen woody debris was noted. Woody debris size was categorized based on its diameter as fine (<2 cm), small (2 cm), medium (4 cm), large (6 cm), and extra-large (>10 cm).

3.1.2. Ground measurements for mangrove forest structure and volume

Ground measurements of three-dimensional (3D) mangrove forest structure and volume were made using a terrestrial laser scanning system to (i) supplement field plot-based forest inventory data and (ii) provide surface area estimates for scaling chamber flux measurements. These 3D measurements provide information on stem density, vertical distributions of biomass, and stand volume and surface area. A terrestrial scanning RIEGL VZ-400i instrument and

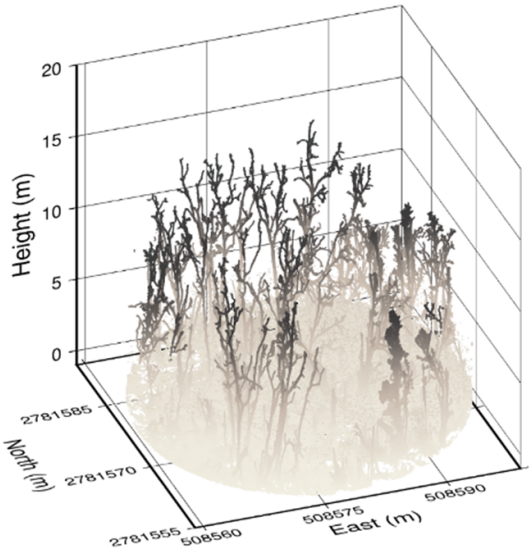

Figure 3. Example of a terrestrial laser scan of the mangrove 'ghost forest' ecosystem at Flamingo, Everglades National Park. The scan provides information on mangrove structure, including density and vertical profiles, as well as volume information that can be used to estimate biomass.

two Global Navigation Satellite System (GNSS) units are used to collect lidar point cloud data in the field (figure 3). The integrated GNSS-TLS system has been optimized in the lab and through prior studies and its performance is robust for coastal systems (Xin *et al* 2017, Xiong *et al* 2017, 2019). The scanner is programmed to measure distances by emitting a high frequency of laser pulses and capturing the return pulses when they are reflected from the surfaces of objects. The wavelength of the laser pulses is 1550 nm and the pulse rate can be up to 1200 kHz. The range measurement for the scanner can be as far as 880 m with an accuracy of 5 mm. The field of view is 360° in the horizontal plane and 100° in the vertical plane.

In each field plot, four panorama scans are collected around the center of the plot to reduce occlusion effects from branches and stems. Each scan takes ∼47 s and provides about 24 million points. The scan resolution is set to be 0.03 degree in both horizontal and vertical directions. A Trimble R8 GNSS unit was mounted on the scanner and used as a rover station. The other GNSS unit, a Trimble R6, is set up as a base station near the field plot. The observation time for the base station exceeds 4 h each day providing centimeter-scale accuracy. During each scan, the position of the scanner is measured by R8 with Real-Time Kinematic (RTK) method. In post-processing, point clouds from each scan is registered in a local 'project' coordinate system by automatic data registration method in RISCAN PRO software. The core methodology is to apply an Iterative Closest Point (ICP) method in overlapped areas between multiple scans (Chen and Medioni 1992). The registered point cloud are georeferenced with the GNSS coordinates of four scan positions. Standard errors for registration and georeferencing are expected to be under 1 cm. The horizontal coordinates are WGS 84/UTM zone 17 N and the vertical datum is Earth Gravitational Model 96 (EGM96) geoid. On order of 50–100 scans will be made in a mix of mangrove stands (from healthy to dead or dying) based on landscape position and disturbance history.

3.1.3. Ground measurements: mangrove species composition

Vegetation spectral reflectance provides biophysical information that can be used to understand and infer species composition, vegetation health, phenology, and sub-canopy water and soil properties. Leaf-level measurements of the spectral reflectance of the main plant species and soil and water surfaces across Southern Florida will be archived in a local database. The Analytical Spectral Devices, Inc. (ASD) FieldSpec Pro. spectroradiometer was used to acquire visible, near-infrared, and short-wave infrared spectra ranging from 350 to 2500 nm at 10 nm resolution, through a fiber cable. The absolute reflectance of classes of trees, grasses, shrubs, soil, and water were calculated with target object measurements divided by a simultaneous white panel measurement. The sensor probe uses a 25° view angle, at about 30 cm distance from the target object, to collect sample spectra at selected sites of vegetation and soil within 'ghost' mangrove stands, healthy mangroves with gaps, inundated grass, or shrubs. Reflectance samples were measured at four different positions from the sun, one on top (nadir) and three at different sun angles. For each position, the device recorded the average of 25 discrete measurements. Each reflectance measurement was normalized for incoming solar radiation using the reflectance of a white Spectralon panel. All measurements were taken under a clear sky or with as few clouds as possible. The absolute reflectance of a sample was calculated by averaging the spectral values taken at the four sun angle positions of an object. Plots of selected samples and corresponding reflectances are shown in figure 4.

3.1.4. Ground measurements: soil and vegetation fluxes with chambers

The methods for estimating GHG fluxes have been relatively well-established for quantifying soil, water, root, and stem exchange with the atmosphere. However, the relative contribution of these components to the overall ecosystem flux is still an active area of research. For example, recent studies have shown that gas fluxes from tree stems can be equally as relevant to the total ecosystem budget (Pangala *et al* 2013, 2015, 2017). A study by Jeffrey *et al* (2019) found that methane fluxes from Australian mangroves themselves are also considerable relative to the overall ecosystem budget. In 2022, researchers published similar data that provided the first evidence that the aerial pneumatophore roots of mangroves, specifically for

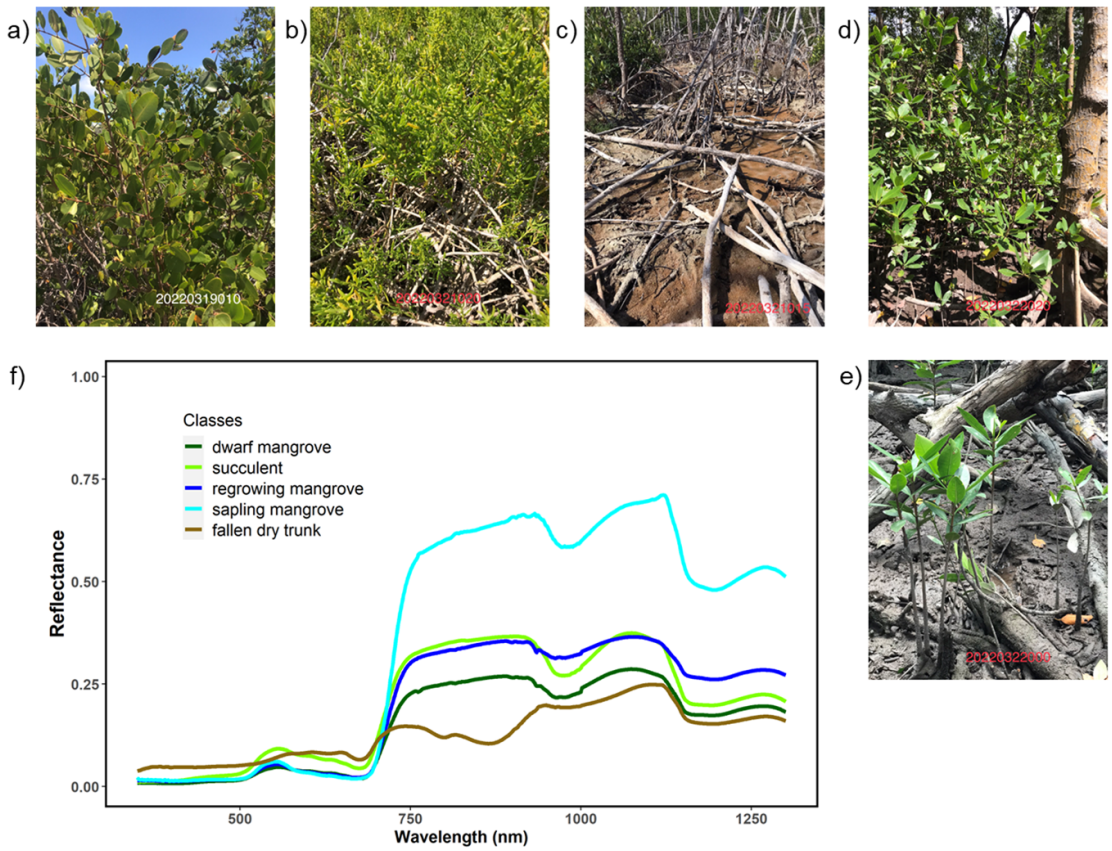

Figure 4. Spectral reflectance curves of the field-measured data: field pictures of (a) a dwarf mangrove, (b) succulent, (c) fallen dry trunks of dead mangroves, (d) regrowing young mangroves in a gap of a healthy mangrove forest, (e) mangrove saplings in the gap, and (f) corresponding reflectances measured by ASD spectrometer.

Avicennia marina, released 84% of the total ecosystem methane (Zhang *et al* 2022).

In the first BlueFlux field campaign, tree, root, and soil CO_2 and CH_4 fluxes were measured in March 2022 at two highly degraded and two intact/regenerating forest sites within Everglades National Park (figure 5). Fluxes were measured within plots previously scanned for forest structure and volume (section 3.1.2) to allow for scaling of areal fluxes from ecosystem components to stand-level totals. Hand-made plastic chambers fitted with an inlet, outlet and a vent were used to measure the change of methane concentration over time from different plant and soil components. The Ultraportable Los Gatos Research Methane Analyzer and the portable Picarro GasScouter G4301 Mobile Gas Concentration Analyzer backpack were used to measure 1 Hz high-resolution CH_4 and CO_2 concentrations. Various chamber shapes were assembled and employed to account for the variety of shapes and sizes of the plant and sediment components (figure 5; Troxler *et al* 2015, Zhang *et al* 2022), with the volume of each chamber calculated empirically by dilution of a methane standard (Siegenthaler *et al* 2016, Jeffrey *et al* 2020). These chambers included a ventilation hole to reduce pressure upon the surface when pushing and securing the chamber to the tree stem, soil, and root surfaces. This was plugged up with a rubber stopper after the chamber was affixed to the tree. Stem and prop root chambers were sealed directly to the plant surface using Amaco potting clay. Pneumatophore chambers enclosed a single pneumatophore, with neoprene foam and potting clay used to seal around the base. Soil chambers were sealed, using Dow Corning vacuum grease, to 8 inch diameter PVC collars, which were previously inserted 2 cm into the sediment at least 1 h prior to sampling in order to avoid interference from sediment degassing. Chambers were tested for leaks using CO_2 readings prior to each measurement.

At each site, for sediment measurements, ten collars were distributed randomly around the plot. Further, a minimum of five standing stems were measured, for both living trees and snags. Stem fluxes were measured at 0, 50, and 100 cm from the base of the tree in order to test for vertical gradients in stem efflux, which can be indicative of soil rather than stem origin of stem-emitted gasses (Barba *et al* 2019). For red mangrove stems, an additional flux was measured at the base of a live prop root. For black mangrove stems an additional flux was measured on an adjacent pneumatophore. For each stem, a variety of ancillary data were also collected, including DBH, perimeter at each measurement height, tree stem, soil,

Figure 5. Diagram of ecosystem component fluxes measured via static chamber method and photographs of corresponding static chamber designs used: (a) pneumatophores, (b) mangrove stems, (c) sediments, (d) prop roots.

and air temperature. Chamber incubations occurred for a minimum of 2 min for soils and 3 min for plant components.

3.1.5. Ground measurements: water chemistry

To capture water-to-air GHG exchange and its variability in mangrove waters in the Florida Everglades, a three-day spatial survey (March 2022) was conducted by navigating a houseboat from Coot Bay (25.18°N, 80.91°W), up the Joe River to the Shark River to Tarpon Bay and back while measuring pH, water temperature, salinity, CO_2 and CH_4 and N_2O concentrations, and CO_2 and CH_4 stable isotopes. Surface water was pumped continuously from ~0.5 m water depth to the on-board setup consisting of a 'showerhead' equilibrator that was connected via a closed air loop to two GHG gas analyzers, a Picarro G2201*i* and a Picarro G2308. (cavity ring-down spectroscopy) measuring continuous high-resolution CO_2, CH_4, and N_2O concentrations (ppm) Surface-water conductivity (EC), dissolved oxygen (DO), temperature, pH, and colored dissolved organic matter (CDOM) were measured every minute using a calibrated multiparameter sonde (Eureka Water Probes). Filtered sterilized discrete samples for spectrophotometric pH, dissolved inorganic carbon (DIC) and total alkalinity (Talk) were collected periodically and analyzed in the laboratory at Yale University.

3.1.6. Ground measurements: long-term carbon burial

Blue carbon stocks include the total amount of carbon buried in soil and within living and non-living biomass, both above- and below-ground, in blue carbon ecosystems (Windham-Meyers *et al* 2019). Long-term blue carbon burial can be estimated by multiplying the sediment accumulation rate measured from the decay of ^{210}Pb below the surface mixed layer (usually below 30 cm depth) by the burial concentration of organic carbon (from depth profile of organic carbon). Included in this is the active uptake and preservation of CO_2 within the ecosystem (referred to as carbon sequestration) as well as the long-term (>100 year; e.g. Fearnside 2002) accumulation and burial of carbon pools belowground (referred to as blue carbon storage). To better understand variability in blue carbon sequestration and storage in mangroves forests within the Everglades, we collected 1 m sediment cores using Russian peat borers that will be measured for total organic carbon (TOC) and for radioactive isotopes (^{210}Pb for <100 year carbon sequestration and ^{14}C for >100 year carbon burial and storage). While many studies estimate carbon stocks using carbon inventories alone (i.e. TOC), radioactive isotopes are needed to understand variability in sedimentation and will provide a better understanding of the timescales associated with blue carbon storage development in the mangrove forests.

3.1.7. Ground measurements: flux tower observations
The eddy covariance (EC) method was used to measure the exchange of trace gasses (CO_2 and CH_4) between wetland systems and the atmosphere throughout the Florida Everglades. Several flux towers exist in the region as part of the FCE LTER along the Shark River Slough (SRS) and Taylor Slough/Panhandle (Ts/Ph) hydrologic gradients (Malone *et al*, 2015). The EC towers are equipped with 3D sonic anemometers (model RS-50, Gill Co., Lymington, England) that measure wind speed and virtual temperature, and use an open path infrared CO_2/H_2O gas analyzer (LI-7500, LI-COR, Inc., Lincoln, Nebraska), and a CH_4 analyzer (LI-7700, LI-COR Inc., Lincoln, Nebraska). Flux data are measured at 20 Hz. In addition to flux data, meteorological measurements include net radiation (CNR 1, Kipp and Zonen, Bohemia, New York) and incoming and reflected PAR (model LI-190SB, LI-COR, Inc., Lincoln, Nebraska), air temperature (T_a) and humidity (HMP45C, Campbell Scientific, Inc., Logan, Utah) and wind speed and direction (model 05103 RM Young, Traverse City, Michigan).

The original riverine mangrove forest tower, SRS6, was constructed in June of 2003 and the instruments were installed 27 m above the soil surface on a 30 m tower. While measurements of CO_2 and H_2O go back to 2004, CH_4 measurements began in 2018. Air temperature is measured at 20, 15, 11, 6, and 1.5 m above the ground surface using aspirated and shielded thermometers (107 temperature probes, Campbell Scientific, Inc.). Below ground soil heat flux (HFT 3.1, Campbell Scientific, Inc.) and soil temperature (105 T, Campbell Scientific, Inc.) (T_s) are measured at 5, 10, 20, and 50 cm. Hydrologic data at this site are continuously monitored and recorded every 15 min at a station 30 m south of Shark River and 150 m west of the flux tower. Measurements included specific conductivity and temperature (600 R water quality sampling sonde, YSI Inc., Yellow Springs, Ohio) of surface well water and water level (Waterlog H-333 shaft encoder, Design Analysis Associates, Logan, Utah). The detailed information on construction of base of tower and other supporting structure can be found in Barr *et al* (2010).

3.2. Airborne EC fluxes

Airborne EC (AEC) is a well-established technique for quantifying surface-atmosphere exchange of trace gasses and energy (Desjardins *et al* 1982). When combined with wavelet transforms (Wolfe *et al* 2018), AEC can characterize spatial gradients in fluxes at model-relevant scales (1–100 km). Flux footprint modeling allows for evaluation of fluxes within the context of surface properties and modeled fluxes (Hannun *et al* 2020, Vaughan *et al* 2021). Such data is complementary to ground-based observations, which integrate over a relatively small area but may better constrain site-specific processes and temporal variability.

BlueFlux AEC observations employ the NASA CArbon Atmospheric Flux Experiment payload on a Beechcraft King Air A90 flown by Dynamic Aviation and equipped with meteorological and trace gas sensors. An AIMMS-20 (Aventech) provides 10 Hz observations of 3D wind velocities, air temperature, aircraft position, and aircraft orientation (pitch/roll/yaw). This system includes a probe (mounted under the left wing) for meteorological measurements coupled with high-resolution differential GPS and inertial navigation systems. Similar systems have been utilized for airborne EC previously (Vaughan *et al* 2021). Ambient air is sampled through a gas inlet mounted under the right wing and transferred through a Teflon PFA tube (in the wing) to two gas sensors in the cabin. Based on analysis of cospectra, the size of flux-carrying eddies are 100–3000 m, much larger than the 15 m of space between the inlet and wind sensor. A Picarro G2401 m provides 0.5 Hz measurements of CO_2, CH_4, H_2O, and CO, while a Picarro G2311-f provides 10 Hz measurements of CO_2, CH_4, and H_2O. The G2401 m contains specialized pressure control systems for airborne operation and thus serves as the accuracy standard for mixing ratios, while the G2311-f provides the fast time response needed for AEC. Dry CO_2 and CH_4 mixing ratios are calibrated in the laboratory against NOAA World Meteorological Organization compressed gas standards with a two-point calibration.

Figure 6 maps the flight tracks from the April 2022 field campaign. Each deployment consists of 4–6 flights (25 flight hours per deployment), with five deployments planned over 2022 and 2023. The flights are designed to focus on coastal mangrove vegetation in South Florida but also include mapping over inland forests and wetlands, such as the extensive sawgrass marshes (*Cladium jamaicense*). The deployments are scheduled to capture seasonal and interannual variation, as well as diurnal changes, while taking into account flight safety due to weather, i.e. late-afternoon storms, hurricane season, and other flight-path restrictions. Flight duration ranges from 2.5 to 4.5 h. Typical altitude is 100 m above ground level, with occasional spirals to ascertain mixed layer depth and flux legs higher in the mixed layer (200–800 m) to determine vertical flux divergence corrections. At an altitude of 100 m and typical surface wind speeds of 5–10 m s^{-1}, we expect 50% of the flux footprints to fall within 1000 m upwind and 90% within 5000 m. On two representative legs spanning inland forest, mangroves, and freshwater marsh, fluxes for CO_2 ranged from 0 to -40 μmol CO_2 m^{-2} s^{-1} and fluxes for CH_4 ranged from 0 to 200 nmol CH_4 m^{-2} s^{-1}

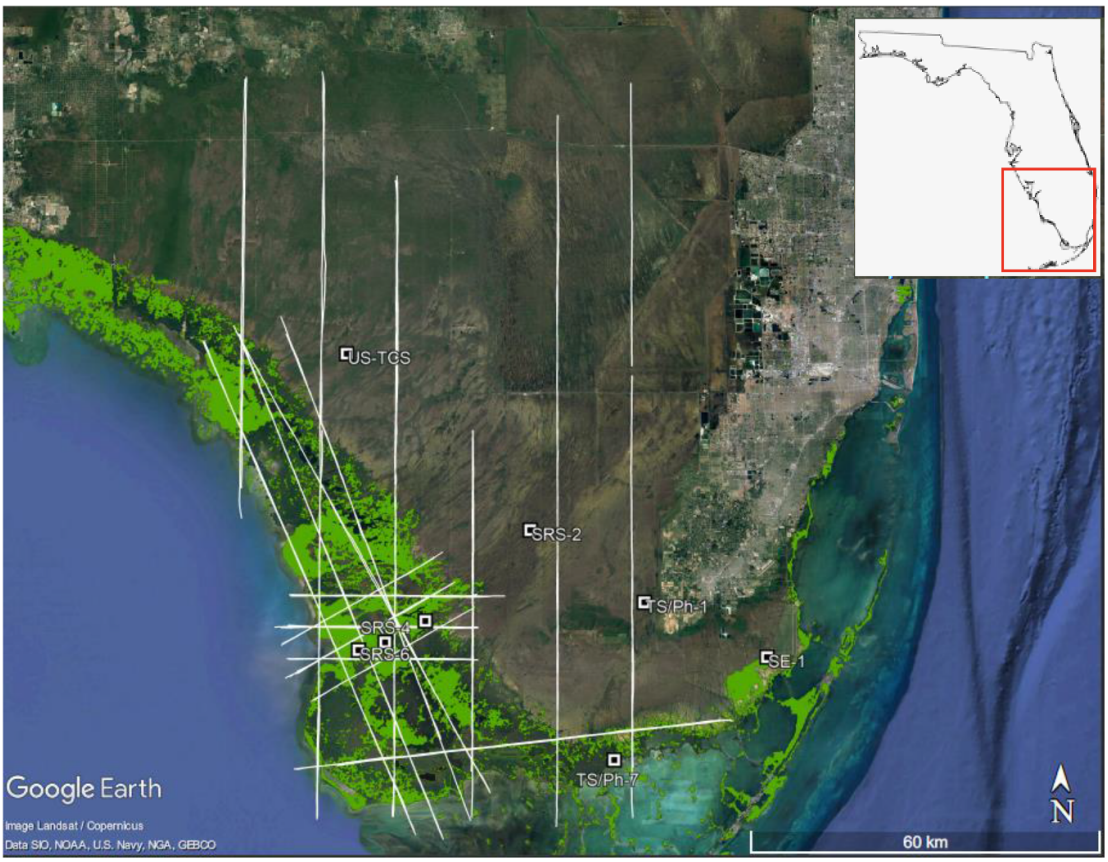

Figure 6. BlueFlux airborne operations in April 2022. White lines show tracks for airborne flux legs; note that each line may include multiple overlapping transects. White squares are long-term surface observation sites. Green patches denote Mangrove extent as of January 2022 (https://geodata.myfwc.com/datasets/myfwc::mangrove-habitat-in-florida-1/about, last accessed 21 June 2022) and the location of the SRS and TS flux towers are labeled. Inset shows the location of the operation area in Southern FL.

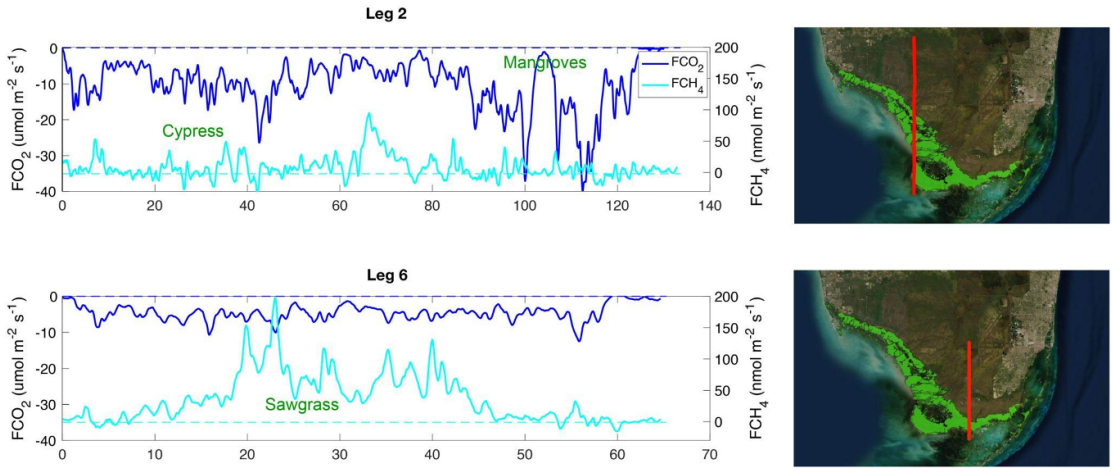

Figure 7. Time series of methane (cyan) and carbon dioxide (blue) fluxes on two legs of the Everglades raster flight from 21 April 2022. The *x*-axis is the distance traveled over each leg, with 0 denoting the northernmost point of each leg. Maps to the right of the time series depict the flight tracks of each leg in red. Green shading shows regions of mangrove habitats. The wind during this flight was from the northeast at an average of 9 ± 2 m s^{-1}.

(figures 7(a) and (b)). In general, the methane fluxes appear to be higher for sawgrass and CO_2 uptake greater for mangroves for the April field campaign. Further flights and analysis will explore seasonal and interannual variability.

3.3. Prototype carbon flux and blue carbon products

The airborne flux measurements will be used as training data for a data-driven upscaled model that will provide daily gridded CH_4 and CO_2 fluxes

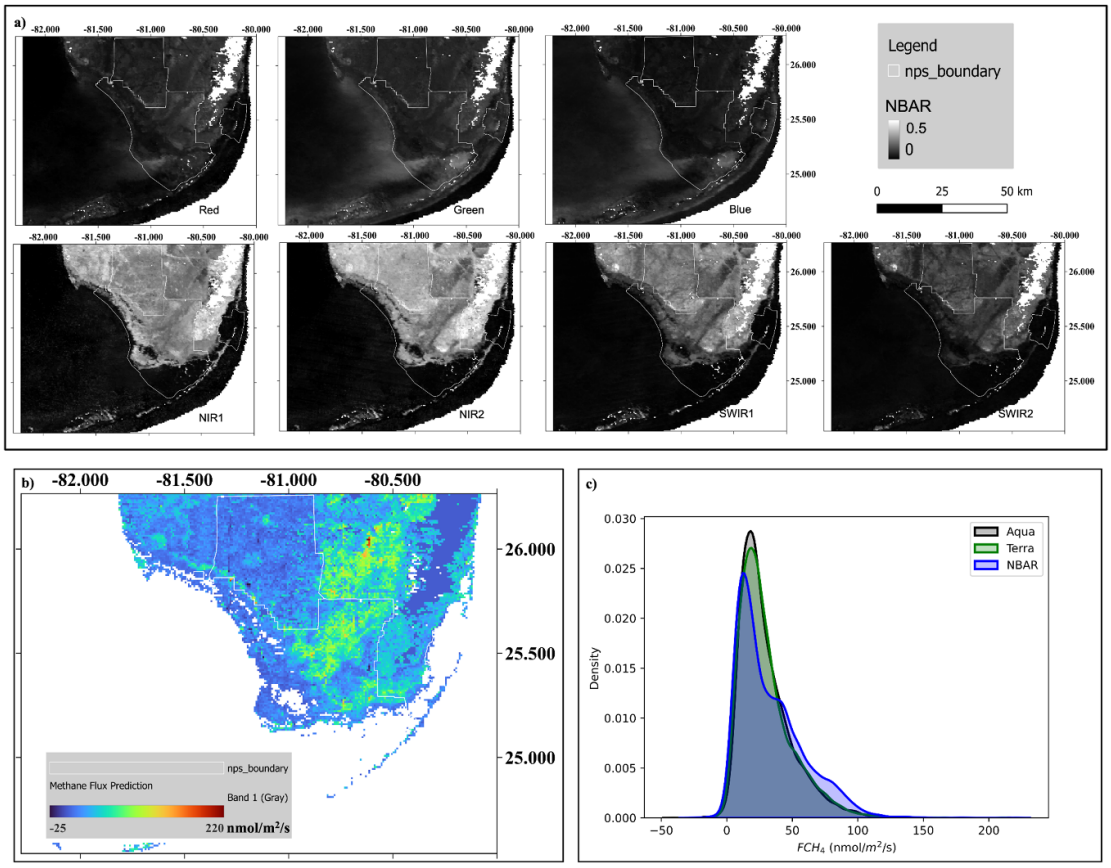

Figure 8. Data-upscaling for methane using flight tracks in figure 6 to train a reflectance-based model using (a) MODIS NBAR of all seven land bands: red (620–670 nm), green (545–565 nm), blue (459–479 nm), NIR1 (841–876 nm), NIR2 (1230–1250 nm), SWIR1 (1628–1652 nm), SWIR2 (2105–2155 nm). The Everglades National Park boundary is shown in white polygons; (b) the gridded methane fluxes for April 2022; and (c) comparison between modeled fluxes from MODIS NBAR reflectance versus Terra and Aqua.

to be compared with the long-term burial rates. Given the extensive spatial and temporal coverage of the fluxes from the flights, and combined with the disaggregation of the ecosystem level fluxes to the components of water, soil and stem, and the validation with tower data, the gridded prototype products can provide the basis for a variety of studies. Figure 8 shows an example of gridded methane fluxes using training data from the seven flight days between 19th and 26th April 2022. These flights provided measurements of methane fluxes for 43 141 sample points at 500 m spatial resolution. We used the MODIS Nadir Bidirectional Reflectance Distribution Function (BRDF)-Adjusted Reflectance (NBAR, MCD43A4v006) data over the study area downloaded from Google Earth Engine. MODIS NBAR is developed daily at 500 m spatial resolution, using 16 d of Terra and Aqua data to remove view angle effects and temporally weighted to the ninth day as the best local solar noon reflectance (Schaaf *et al* 2002, Wang *et al* 2018).

Mean values of MODIS NBAR product between 19th and 26th April were composited per band of seven spectral bands (figure 8(a); red, NIR1, blue, green, NIR2, SWIR1, SWIR2) as model input features. The MODIS Terra land-water mask (MOD44Wv006, Carroll *et al* 2017) of 2015 was applied to mask open-water pixels. Sampling points from the flight lines were mapped to the MODIS grid cells by averaging FCH_4 and FCO_2 values of points that fell in the same MODIS pixel. This produced 1528 gridded data. An upscaling model was trained at the MODIS pixel scale using ensemble random forest regressors (Breiman 2001, Kim *et al* 2020). Random forest regression contains an assembly of independent trees constructed from a random subset of input data or input space (features). The generalization error converges as the forest grows to a limit, which avoids overfitting. We used the scikit-learn library in Python to build up random forest regressors with a bootstrap ensemble sampling for data. A 'tree' grew a split where a random selection of two features reduces the mean squared error (MSE) at a leaf node.

Red and near-infrared bands that have been widely used for characterizing vegetation chlorophyll, canopy structure and soil wetness were among the most important bands to model spatial variability of methane and carbon dioxide fluxes in the Everglades National Park and surrounding region. We also trained separate upscaling models on MODIS Aqua

and Terra 8 day composite Level 3 surface reflectance data (MYD09A1v061 and MOD09A1v006, Vermote *et al* 2002, Bréon and Vermote 2012). Only pixels with good quality data were used. The RMSE of the Aqua model was 12.74 nmol m^2 s^{-1} and 12.41 nmol m^2 s^{-1} for Terra trained model, compared with 10.1 nmol m^2 s^{-1} for the NBAR product. Methane fluxes mapped from NBAR data in our study area have a better spatial representation of methane emission gradients and variabilities than those from Aqua or Terra data (figure 8(c)). High methane emissions were located in inundated sawgrass marsh in the SRS and the estuarine section of Taylor Slough (figure 8(b)). Due to frequent cloud cover, the 8 day composite of Aqua or Terra data are noisier than the NBAR product over high emission marsh and low emission cypress swamp, which produced different density distributions of methane fluxes (figure 8(c)). Future work will consider how to integrate sub-daily and sub-weekly tidal and meteorological information not included in the Aqua and Terra products.

4. Anticipated results

One of the main concerns regarding 'blue carbon' as an NBS is that it considers carbon stores and long-term burial rates but overlooks non-CO_2 GHG emissions that can affect (positively or negatively) the overall net radiative forcing effect of these ecosystems (Malerba *et al* 2022). Mangroves are intertidal ecosystems and while net autotrophic at the ecosystem scale (Duarte *et al* 2005, Alongi 2014), creek waters and sediments are generally a source of atmospheric CO_2 and CH_4 (Call *et al* 2015, Rosentreter *et al* 2018a) and can also act as a source or sink for N_2O (Maher *et al* 2016, Reithmaier *et al* 2020). Along the tidal elevation gradient (creek to forest basin), mangrove coverage, species diversity, and sediment structure can change markedly, resulting in great spatial variability of GHG fluxes. The tidal systems also have large differences at diurnal time scales, which BlueFlux will address by integrating high-density timeseries from the flux towers with the more spatially expansive aircraft flux observations.

Using the upscaled methane and carbon dioxide fluxes from the NBAR-based reflectance model, we estimated for the Everglades National Park (~6000 km^2) that CO_2 removals were 91 677 Mt d^{-1} or 33.5 Tg CO_2 y^{-1} and CH_4 emissions were 182.7 Mt d^{-1} or 0.06 Tg CH_4 yr^{-1} (where Tg = teragram = 1×10^{12} grams). To compare how much methane emissions reduces the climate mitigation potential of carbon dioxide removals, we apply the Intergovernmental Panel on Climate Change (IPCC) 100 year global warming potential of 28 and estimate that 1.7 Tg CH_4-CO_2-eq yr^{-1} are emitted to the atmosphere. This suggests that about 5% of the CO_2 uptake by vegetation is offset by methane emissions. Subsequent field campaigns and modeling will integrate seasonal and inter-annual variability into these estimates as well as address and quantify the sources of uncertainty related to local and long-distance lateral fluxes and long-term carbon burial. Our upscaled estimate is similar order of magnitude to Troxler *et al* (2013) who also partition how much of the carbon removed from the atmosphere is transported laterally via aquatic fluxes to the Gulf of Mexico.

The BlueFlux field campaign is designed to collect detailed information on mangrove structure with multi-scale measurements of GHG fluxes. The data-upscaling approach described in section 3.3 will capture a variety of edaphic, hydrologic and disturbance gradients either through the reflectance data or through additional covariates, such as wind speed, remote-sensed forest structure using radar or lidar, and topographic information. By combining flux tower measurements that provide sub-daily time series with aircraft measurements that cover large spatial variability, the processes driving GHG fluxes can be incorporated into upscaled models. The gridded carbon flux products will provide a basis for evaluating trends over the past two decades in GHG fluxes and their spatial patterns in response to changing climate and climate extremes, hurricane history, and land management.

5. Anticipated impact

Blue carbon is integrated within many policy-guiding documents and climate mitigation policies themselves (Hilmi *et al* 2021). The IPCC Good Practice Guidelines for wetland inventories (IPCC 2014) and the Special Report on the Ocean and Cryosphere in a Changing Climate both discuss the consequences of maintaining and restoring these ecosystems for climate mitigation. The Blue Carbon Policy Project of the International Union for the Conservation of Nature helped guide recommendations to the United Nations Framework Convention on Climate Change's 26th Conference of Parties (COP26) in 2021. At COP26, blue carbon related goals included enhancing ambition, accelerating implementation and monitoring and verification of results.

A key aspect of NASA's CMS is to support stakeholder needs and expand partnerships with practitioners involved with climate mitigation. BlueFlux is partnered with stakeholders in (1) the private sector through the Everglades Foundation and the Environmental Leadership and Training Initiative at Yale University, (2) through federal agencies, including NASA, United States Geological Survey, the National Park Service, and National Science Foundation, (3) through tribal nations, including the Miccosukee, the Seminole Nation of Oklahoma and the Seminole Tribe of Florida, and (4) through international partnerships with the Coastal Biodiversity Resilience to increasing Extreme events in Central

America. The data access policy follows NASA's Open Source Science philosophy of being freely and readily accessible, with transparent metadata and documentation.

BlueFlux intends to benefit these stakeholders by accounting for GHG exchanges from critical blue carbon ecosystems, i.e. mangroves and sawgrass marshes. The multi-source, multi-scale quality of the project also aims to allow stakeholders to access information and data from the soil, and water to the atmosphere that may support the generation and refinement of IPCC Tier 3 inventory methods, and the assessment and reduction of the uncertainties associated with current models for NGHGI (Ogle *et al* 2019). For example, the IPCC 2013 Supplement for wetlands currently uses a single emissions factor of 19.37 g CH_4 m^2 y^{-1} for wetland cases where salinity is <18 parts per thousand (ppt) and zero for when salinity is >18 ppt (IPCC 2014) and assumes no methane emissions for mangrove systems. Our study will help better understand how disturbance, hydroperiod and salinity gradients drive methane emissions and help provide a basis for Tier 3 approaches where relevant.

The cross-scale calibrated BlueFlux products, developed at 500–1000 m resolution for Mesoamerica and the Caribbean might also support local, and regional policies and projects on climate change adaptation and mitigation, ecosystem restoration, and carbon market. The project also provides data that can support the Global Stocktake of the Paris Agreement (GST) and the nationally determined contributions process, since it maps GHG flux time series from coastal ecosystems under varying conditions and, as consequence, highlights the history of regional carbon sinks and sources.

Data availability statement

No new data were created or analysed in this study.

Acknowledgments

The BlueFlux project acknowledges core support from the NASA Carbon Monitoring System and NASA's Terrestrial Ecology Program. We would like to thank the BNP-PARIBAS foundation for their support to the CORESCAM project (Coastal and Marine biodiversity resilience to increasing extreme events in Central America and the Caribbean), from their 2019 Biodiversity and Climate Change call. We also thank the Everglades and Big Cypress National Parks and the Florida Coastal Everglades Long Term Ecological Network for their support. We thank Dr Christopher Holmes (Florida State University) for providing airborne support and Dr Brad Eyre (Southern Cross University, Australia) for providing helpful comments on an earlier draft of this manuscript.

ORCID iDs

Benjamin Poulter https://orcid.org/0000-0002-9493-8600
Francis M Adams-Metayer https://orcid.org/0000-0003-1483-7963
Cibele Amaral https://orcid.org/0000-0001-7597-2427
Abigail Barenblitt https://orcid.org/0000-0002-9758-2670
Anthony Campbell https://orcid.org/0000-0001-8379-9513
Sean P Charles https://orcid.org/0000-0002-5626-1192
Rosa Maria Roman-Cuesta https://orcid.org/0000-0002-6945-8402
Erin R Delaria https://orcid.org/0000-0002-6033-848X
Cheryl Doughty https://orcid.org/0000-0003-3802-9813
Temilola Fatoyinbo https://orcid.org/0000-0002-1130-6748
Jonathan Gewirtzman https://orcid.org/0000-0003-3959-3758
Thomas F Hanisco https://orcid.org/0000-0001-9434-8507
Reem Hannun https://orcid.org/0000-0001-5195-5307
David Lagomasino https://orcid.org/0000-0003-4008-5363
Leslie Lait https://orcid.org/0000-0002-8363-859X
Sparkle L Malone https://orcid.org/0000-0001-9034-1076
Paul A Newman https://orcid.org/0000-0003-1139-2508
Peter Raymond https://orcid.org/0000-0002-8564-7860
Judith A Rosentreter https://orcid.org/0000-0001-5787-5682
Nathan Thomas https://orcid.org/0000-0002-7808-6444
Derrick Vaughn https://orcid.org/0000-0003-1178-259X
Glenn M Wolfe https://orcid.org/0000-0001-6586-4043
Lin Xiong https://orcid.org/0000-0002-9703-7189
Qing Ying https://orcid.org/0000-0002-9752-8973
Zhen Zhang https://orcid.org/0000-0003-0899-1139

References

Adame M F, Santini N S, Torres-Talamante O and Rogers K 2021 Mangrove sinkholes (cenotes) of the Yucatan Peninsula, a global hotspot of carbon sequestration *Biol. Lett.* **17** 5
Alongi D M 2014 Carbon cycling and storage in mangrove forests *Ann. Rev. Mar. Sci.* **6** 195–219
Alvarado-Barrientos M S, López-Adame H, Lazcano-Hernández H E, Arellano-Verdejo J and

Hernández-Arana H A 2021 Ecosystem-atmosphere exchange of CO_2, water, and energy in a basin mangrove of the Northeastern Coast of the Yucatan Peninsula *J. Geophys. Res. Biogeosci.* **126** e2020JG005811
Barba J *et al* 2019 Methane emissions from tree stems: a new frontier in the global carbon cycle *New Phytol.* **222** 18–28
Barr J G, Engel V, Fuentes J D, Zieman J C, O'Halloran T L, Smith T J III and Anderson G H 2010 Controls on mangrove forest-atmosphere carbon dioxide exchanges in Western Everglades National Park *J. Geophys. Res. Biogeosci.* **115** G0205
Breiman L 2001 Random Forests *Mach. Learn.* **45** 5–32
Bréon F-M and Vermote E 2012 Correction of MODIS surface reflectance time series for BRDF effects *Remote Sens. Environ.* **125** 1–9
Call M *et al* 2015 Spatial and temporal variability of carbon dioxide and methane fluxes over semi-diurnal and spring–neap–spring timescales in a mangrove creek *Geochim. Cosmochim. Acta* **150** 211–25
Carroll M L, DiMiceli C M, Townshend J R G, Sohlberg R A, Elders A I, Devadiga S, Sayer A M and Levy R C 2017 Development of an operational land water mask for MODIS collection 6, and influence on downstream data products *Int. J. Digit. Earth* **10** 207–18
Cavanaugh K C, Kellner J R, Forde A J, Gruner D S, Parker J D, Rodriguez W and Feller I C 2014 Poleward expansion of mangroves is a threshold response to decreased frequency of extreme cold events *Proc. Natl Acad. Sci.* **111** 723–7
Chen Y and Medioni G 1992 Object modelling by registration of multiple range images *Image Vis. Comput.* **10** 145–55
Delwiche K B *et al* 2021 FLUXNET-CH_4: a global, multi-ecosystem dataset and analysis of methane seasonality from freshwater Wetlands *Earth Syst. Sci. Data* **13** 3607–89
Desjardins R L, Brach E J, Alvo P and Schuepp P H 1982 Aircraft monitoring of surface carbon dioxide exchange *Science* **216** 733–5
Duarte C M, Losada I J, Hendriks I E, Mazarrasa I and Marbà N 2013 The role of coastal plant communities for climate change mitigation and adaptation *Nat. Clim. Change* **3** 961–8
Duarte C M, Middelburg J J and Caraco N 2005 Major role of marine vegetation on the oceanic carbon cycle *Biogeosciences* **2** 1–8
Fearnside P M 2002 Why a 100-year time horizon should be used for global warming mitigation calculations *Mitig. Adapt. Strat. Glob. Change* **7** 19–30
Forster P *et al* 2021 Chapter 7: the earth's energy budget, climate feedbacks, and climate sensitivity *Climate Change 2021: The Physical Science Basis. Contribution of Working Group I to the Sixth Assessment Report of the Intergovernmental Panel on Climate Change* (https://doi.org/10.1029/2020GL091883)
Goldberg L, Lagomasino D, Thomas N and Fatoyinbo T 2020 Global declines in human-driven mangrove loss *Glob. Change Biol.* **26** 5844–55
Griscom B W *et al* 2017 Natural climate solutions *Proc. Natl Acad. Sci.* **114** 11645–50
Hannun R A *et al* 2020 Spatial heterogeneity in CO_2, CH_4, and energy fluxes: insights from airborne eddy covariance measurements over the mid-Atlantic region *Environ. Res. Lett.* **15** 035008
Hilmi N, Chami R, Sutherland M D, Hall-Spencer J M, Lebleu L, Belen Benitez M and Levin L A 2021 The Role of Blue Carbon in Climate Change Mitigation and Carbon Stock Conservation *Front. Clim.* **3** 710546
IPCC 2019 Special report on climate change and land—IPCC site (available at: www.ipcc.ch/srccl/)
IPCC 2014 *2013 Supplement to the 2006 IPCC Guidelines for National Greenhouse Gas Inventories: Wetlands* ed T Hiraishi, T Krug, K Tanabe, N Srivastava, J Baasansuren, M Fukuda and T G Troxler (Geneva: IPCC)
Jeffrey L C, Maher D T, Tait D R and Johnston S G 2020 A Small Nimble *In Situ* Fine-Scale Flux Method for Measuring Tree Stem Greenhouse Gas Emissions and Processes (S.N.I.F.F) *Ecosystems* **23** 1676–89
Jeffrey L C, Reithmaier G, Sippo J Z, Johnston S G, Tait D R, Harada Y and Maher D T 2019 Are methane emissions from mangrove stems a cryptic carbon loss pathway? insights from a catastrophic forest mortality *New Phytol.* **224** 146–54
Kim Y, Johnson M S, Knox S H, Andrew Black T, Dalmagro H J, Kang M, Kim J and Baldocchi D 2020 Gap-filling approaches for eddy covariance methane fluxes: a comparison of three machine learning algorithms and a traditional method with principal component analysis *Glob. Change Biol.* **26** 1499–518
Knox S H, Jackson R B, Poulter B, McNicol G, Fluet-Chouinard E, Zhang Z, Hugelius G and Zona D 2019 FLUXNET-CH4 synthesis activity: objectives, observations, and future directions *Bull. Am. Meteorol. Soc.* **100** 2607–32
Lagomasino D, Fatoyinbo T, Castañeda-Moya E, Cook B D, Montesano P M, Neigh C S R, Corp L A, Ott L E, Chavez S and Morton D C 2021 Storm surge and ponding explain mangrove dieback in Southwest Florida Following Hurricane Irma *Nat. Commun.* **12** 4003
Macreadie P I, Costa M D P, Atwood T B, Friess D A, Kelleway J J, Kennedy H, Lovelock C E, Serrano O and Duarte C M 2021 Blue carbon as a natural climate solution *Nat. Rev. Earth Environ.* **2** 826–39
Maher D T, Sippo J Z, Tait D R, Holloway C and Santos I R 2016 Pristine mangrove creek waters are a sink of nitrous oxide *Sci. Rep.* **6** 25701
Malerba M E, Friess D A, Peacock M, Grinham A, Taillardat P, Rosentreter J A, Webb J, Iram N, Al-Haj A N and Macreadie P I 2022 Methane and nitrous oxide emissions complicate the climate benefits of teal and blue carbon wetlands *One Earth* **5** 1336–41
Malone S L, Barr J, Fuentes J D, Oberbauer S F, Staudhammer C L, Gaiser E E and Starr G 2016 Sensitivity to low-temperature events: implications for CO_2 dynamics in subtropical coastal ecosystems *Wetlands* **36** 957–67
Marc S, Fatoyinbo L, Smetanka C, Rivera-Monroy V H, Castañeda-Moya E, Thomas N and Van der Stocken T 2019 Mangrove canopy height globally related to precipitation, temperature and cyclone frequency *Nat. Geosci.* **12** 40–45
Mcleod E, Chmura G L, Bouillon S, Salm R, Björk M, Duarte C M, Lovelock C E, Schlesinger W H and Silliman B R 2011 A blueprint for blue carbon: toward an improved understanding of the role of vegetated coastal habitats in sequestering CO2 *Front. Ecol. Environ.* **9** 552–60
Nellemann C, Corcoran E, Duarte C M, Valdes L, De Young C, Fonseca L and Grimsditch G 2009 *Blue Carbon. A Rapid Response Assessment* vol 80 (United Nations Environment Programme, GRID-Arendal)
Ogle S M *et al* 2019 Generic methodologies applicable to multiple land-use categories *Refinement to the 2006 IPCC Guidelines for National Greenhouse Gas Inventories* (*Agriculture, Forestry and Other Land Use* vol 4) ed B E Calvo, K Tanabe, A Kranjc, J Baasansuren, M Fukuda, S Ngarize, A Osako, Y Pyrozhenko, P Shermanau and S Federici (Geneva: IPCC) ch 2
Osland M J, Hartmann A M, Day R H, Ross M S, Hall C T, Feher L C and Vervaeke W C 2019 Microclimate influences mangrove freeze damage: implications for range expansion in response to changing macroclimate *Estuaries Coast.* **42** 1084–96
Pangala S R *et al* 2017 Large emissions from floodplain trees close the Amazon methane budget *Nature* **552** 230–4
Pangala S R, Hornibrook E R C, Gowing D J and Gauci V 2015 The contribution of trees to ecosystem methane emissions in a temperate forested Wetland *Glob. Change Biol.* **21** 2642–54
Pangala S R, Moore S, Hornibrook E R C and Gauci V 2013 Trees are major conduits for methane egress from tropical forested Wetlands *New Phytol.* **197** 524–31
Parkinson R W and Wdowinski S 2022 Accelerating sea-level rise and the fate of mangrove plant communities in South Florida, U.S.A *Geomorphology* **412** 108329

Pete B, Rosenqvist A, Hilarides L, Lucas R M and Thomas N 2022 Global mangrove watch: updated 2010 mangrove forest extent (v2.5) *Remote Sens.* **14** 1034

Reithmaier G M S, Ho D T, Johnston S G and Maher D T 2020 Mangroves as a source of greenhouse gases to the atmosphere and alkalinity and dissolved carbon to the coastal ocean: a case study from the everglades National Park, Florida *J. Geophys. Res. Biogeosci.* **125** e2020JG005812

Roe S *et al* 2019 Contribution of the land sector to a 1.5 °C World *Nat. Clim. Change* **9** 817–28

Rosentreter J A *et al* 2021 Half of global methane emissions come from highly variable aquatic ecosystem sources *Nat. Geosci.* **14** 225–30

Rosentreter J A, Maher D T, Erler D V, Murray R H and Eyre B D 2018b Methane emissions partially offset 'blue carbon' burial in mangroves *Sci. Adv.* **4** eaao4985

Rosentreter J A, Maher D T, Erler D V, Murray R and Eyre B D 2018a Factors controlling seasonal CO_2 and CH_4 emissions in three tropical mangrove-dominated estuaries in Australia *Estuar. Coast. Shelf Sci.* **215** 69–82

Saunois M *et al* 2020 The global methane budget 2000–2017 *Earth Syst. Sci. Data* **12** 1561–623

Schaaf C B *et al* 2002 First operational BRDF, albedo nadir reflectance products from MODIS *Remote Sens. Environ.* **83** 135–48

Seddon N 2022 Harnessing the potential of nature-based solutions for mitigating and adapting to climate change *Science* **376** 1410–6

Siegenthaler A, Welch B, Pangala S R, Peacock M and Gauci V 2016 Technical note: semi-rigid chambers for methane gas flux measurements on tree stems *Biogeosciences* **13** 1197–207

Sippo J Z, Lovelock C E, Santos I R, Sanders C J and Maher D T 2018 Mangrove Mortality in a Changing Climate: an Overview *Estuar. Coast. Shelf Sci.* **215** 241–9

Snedaker S C 1982 Mangrove species zonation: Why? *Tasks for Vegetation Science* ed D N Sen and Rajpurohit (The Hague: Dr W Junk)

Taillie P J, Roman-Cuesta R, Lagomasino D, Cifuentes-Jara M, Fatoyinbo T, Ott L E and Poulter B 2020 Widespread mangrove damage resulting from the 2017 Atlantic mega hurricane season *Environ. Res. Lett.* **15** 064010

Troxler T G *et al* 2013 Integrated carbon budget models for the Everglades terrestrial-coastal-oceanic gradient: current status and needs for inter-site comparisons *Oceanography* **26** 98–107

Troxler T G, Barr J G, Fuentes J D, Engel V, Anderson G, Sanchez C, Lagomasino D, Price R and Davis S E 2015 Component-specific dynamics of riverine mangrove CO_2 efflux in the florida coastal everglades *Agric. For. Meteorol.* **213** 273–82

Vaughan A R, Lee J D, Metzger S, Durden D, Lewis A C, Shaw M D, Drysdale W S, Purvis R M, Davison B and Nicholas Hewitt C 2021 Spatially and temporally resolved measurements of no_x fluxes by airborne eddy covariance over greater London *Atmos. Chem. Phys.* **21** 15283–98

Vermote E F, El Saleous N Z and Justice C O 2002 Atmospheric correction of MODIS data in the visible to middle infrared: first results *Remote Sens. Environ.* **83** 97–111

Wang Z, Schaaf C B, Sun Q, Shuai Y and Román M O 2018 Capturing rapid land surface dynamics with collection V006 MODIS BRDF/NBAR/Albedo (MCD43) products *Remote Sens. Environ.* **207** 50–64

Williamson P and Gattuso J-P 2022 Carbon removal using coastal blue carbon ecosystems is uncertain and unreliable, with questionable climatic cost-effectiveness *Front. Clim.* **4** 130

Windham-Meyers L, Crooks S and Troxler T (eds) 2019 *Blue Carbon Primer: The State of Coastal Wetland Carbon Science Practice and Policy* (Boca Raton, FL: CRC Press)

Wolfe G M *et al* 2018 The NASA Carbon Airborne Flux Experiment (CARAFE): instrumentation and methodology *Atmos. Meas. Tech.* **11** 1757–76

Xin Z, Wang G, Bao Y, Xiong L, Guzman V and Kearns T J 2017 Delineating beach and dune morphology from massive terrestrial laser-scanning data using *generic mapping tools J. Surv. Eng.* **143** 04017008

Xiong L, Wang G, Bao Y, Zhou X, Wang K, Liu H, Sun X and Zhao R 2019 a rapid terrestrial laser scanning method for coastal erosion studies: a case study at Freeport, Texas, USA *Sensors* **19** 3252

Xiong L, Wang G and Wessel P 2017 Anti-aliasing filters for deriving high-accuracy DEMs from TLS data: a case study from Freeport, Texas *Comput. Geosci.* **100** 125–34

Zeng Y, Friess D A, Vadya Sarira T, Siman K and Pin Koh L 2021 Global potential and limits of mangrove blue carbon for climate change mitigation *Curr. Biol.* **31** 1737–1743.e3

Zhang C, Zhang Y, Luo M, Tan J, Chen X, Tan F and Huang J 2022 Massive methane emission from tree stems and pneumatophores in a subtropical Mangrove Wetland *Plant Soil* **473** 489–505